Advances in Pharmacology and Pharmacy 13(4): 627-638, 2025 http://www.hrpub.org
DOI: 10.13189/app.2025.130413

Fabrication and Characterization of Sulforaphane Loaded Magnetic Nanoparticles

Raghavendra Kumar Gunda[1,*], A. Vijayalakshmi[2], Prathap Madeswara Guptha[3], Koteswara Rao GSN[4], Kondapuram Parameshwar[5], Madhavi Latha Chennuru[6]

[1]Department of Pharmaceutics, Narasaraopeta Institute of Pharmaceutical Sciences (Autonomous), Narasaraopet, Andhra Pradesh, India
[2]Department of Pharmacognosy, School of Pharmaceutical Sciences, Vels Institute of Science, Technology and Advanced Studies (VISTAS), Pallavaram, Chennai, Tamil Nadu, India
[3]Department of Pharmaceutical Sciences, School of Biotechnology and Pharmaceutical Sciences, Vignan's Foundation for Science, Technology and Research (Deemed to be University), Guntur, India
[4]Department of Pharmaceutics, Shobhaben Pratapbhai Patel School of Pharmacy & Technology Management, SVKM's NMIMS, Mumbai, Maharashtra, India
[5]Department of Pharmaceutics, Guru Nanak Institutions Technical Campus- School of Pharmacy, Hyderabad, Telangana, India
[6]Department of Pharmacology, Sree Venkateswara College of Pharmacy, Nellore, Andhra Pradesh, India

Received June 5, 2024; Revised January 23, 2025; Accepted August 20, 2025

Cite This Paper in the Following Citation Styles

(a): *[1] Raghavendra Kumar Gunda, A. Vijayalakshmi, Prathap Madeswara Guptha, Koteswara Rao GSN, Kondapuram Parameshwar, Madhavi Latha Chennuru , "Fabrication and Characterization of Sulforaphane Loaded Magnetic Nanoparticles," Advances in Pharmacology and Pharmacy, Vol. 13, No. 4, pp. 627 - 638, 2025. DOI: 10.13189/app.2025.130413.*

(b): *Raghavendra Kumar Gunda, A. Vijayalakshmi, Prathap Madeswara Guptha, Koteswara Rao GSN, Kondapuram Parameshwar, Madhavi Latha Chennuru (2025). Fabrication and Characterization of Sulforaphane Loaded Magnetic Nanoparticles. Advances in Pharmacology and Pharmacy, 13(4), 627 - 638. DOI: 10.13189/app.2025.130413.*

Abstract **Objective:** The purpose of the present research work was to develop Sulforaphane loaded magnetic nanoparticles (MNPs) and the effect of prepared magnetic nanoparticle on the enhancement of bioavailability, stability, and dissolution was studied. Sulforaphane (SFP) is a naturally occurring isothiocyanate and chiefly available in broccoli. **Methods:** Magnetic Nanoparticles were prepared by encapsulating herbal drug SFP with iron salts and the prepared magnetic nanoparticles were analyzed by Infrared Spectroscopy, Crystal Analysis, Scanning Electron Microscope (SEM), Thermal Analysis, Drug Loading Efficiency, Magnetic Analysis, Electrical Analysis and Stability Studies. **Results:** The obtained data of the characterization studies reveal that the magnetic nanoparticles (MNPs) have good holding properties. The particles sizes of MNPs measured from High Resolution Scanning Electron Microscopy (HRSEM) were of ideal size range 100 - 250 nm and showed a regular pattern of spherical shape. The Vibrating Sample Magnetism (VSM) results showed that satisfactory value. The pH of the medium has an inverse relationship with the amount of Sulphoraphane released by the MNPs. **Conclusion:** From the results, the current study concludes that the prepared MNPs (four types) are structurally arranged following a good pattern, sufficient amount of elements with good size range over the particle surface, and exhibit magnetic responsiveness which is sufficient for drug target due to an external magnetic field because of its pore volume and large surface area. Dissolution study reveals that the prepared Sulforaphane loaded MNPs of Iron-MCM-41 showed maximum drug release at pH 5.5.

Graphical Abstract

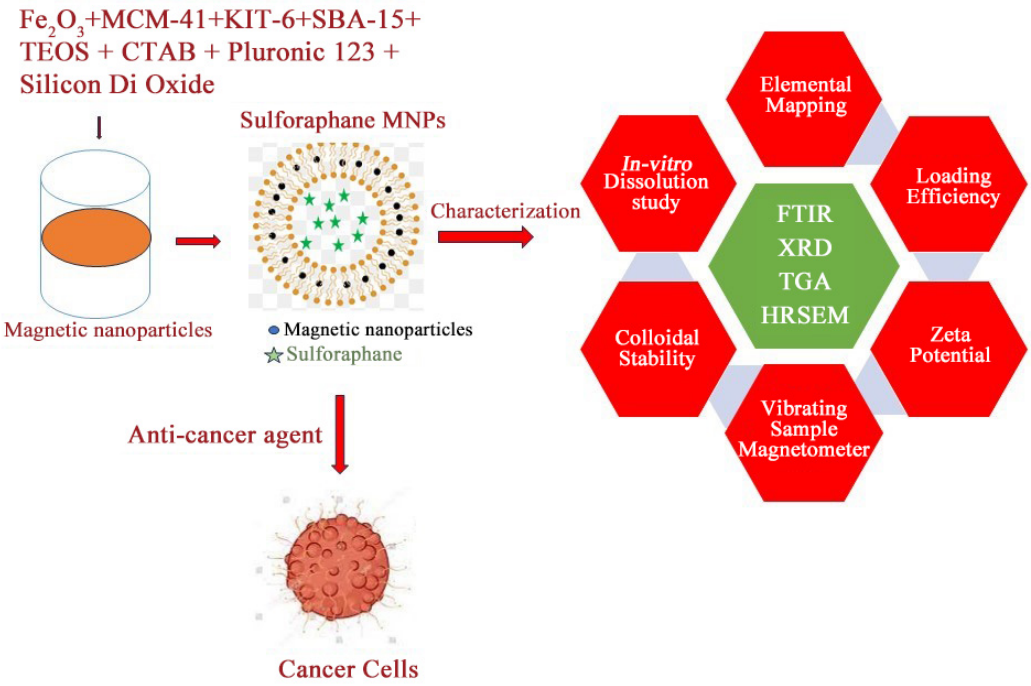

Sulforaphane loaded Magnetic Nanoparticles

Keywords Sulforaphane, Magnetic Nanoparticles, FT-IR, Co-Precipitation Method

1. Introduction

Herbal products were most widely used for various diseases and ailments from ancient period time. Due to its less toxicity and less side effects patients showing interest than allopathic treatment. One more advantage for formulation scientist is compatibility with excipients used for novel delivery systems. Even though having flexibility in all issue, as the same way it has limitation of poor bioavailability and stability issues when compared with modern system of medicine. The drug selected for the proposed study was Sulforaphane.

Sulforaphane, an isothiocyanate occurs naturally and can be found in cruciferous vegetables like broccoli, cauliflower, cabbage, and others (Brussels sprouts). It has potential antineoplastic properties and used for the effective management of Hepatic, Bladder, Prostate, Pancreatic Cancers. It is also shows powerful anticancer activity in case of osteosarcoma and melanoma [1-3]. It shows instability in presence of oxygen, heat and alkaline condition [4, 5].

Oral therapy considered as primary choice for both physicians and patients alike, due its convenience and it improves patient's quality of life. The oral route is preferred for its cost-effectiveness, but it can be limited by various factors such as absorption, bioavailability, protein binding, and metabolism (first-pass effect). These limitations can sometimes overcome by achieving a good clinical outcome, leading to patient non-compliance. The magnetic nanoparticles (MNPs) are promising carriers for the efficient delivery of antineoplastic drugs because there is no burst impact and scaling up is easy. Significantly reduced drug ejection during storage was observed due to high encapsulation of both hydrophilic and lipophilic drug molecules. By changing the lipid matrix, it is possible to modify the drug release profile and noticeably increase stability in the gastro intestinal tract (GIT) at various pH levels [6-8].

The delivery systems containing particles in nano size range (<200 nm) exhibit wide range of benefits for better dissolution, absorption, bioavailability and good clinical outcome. This has been proven in many of chemotherapeutic agents as they produced excellent therapeutic efficacy in animal studies [9].

Magnetic Nanoparticles (MNPs) play an important position in the transport of drug by transporting medications to specific site of the body using external magnetic field. Because of their biocompatibility, ease of surface modification, and magnetic characteristics, MNPs have received a lot of attention in biomedical and industrial applications. Currently the MNPs had attracted interest of researchers in a lot of studies because of the fact of potential biomedical applications such as tissue-specific targeting [10], environmental remediation [11], magnetically tunable colloidal photonic crystals (MTCPC) [12], data storage [13], magnetic resonance imaging (MRI)

[14], micro fluidics [15], material imaging [16], nano fluids [17, 18], optical filters [19, 20], illness sensor [21], magnetic cooling [22, 23], cation sensors [24] and catalysis [25]. Hence the present work is aimed to develop Sulforaphane loaded MNPs with the objective to evaluate the effect of prepared magnetic nanoparticle on the enhancement of bioavailability, stability, and dissolution. The developed MNPs were characterized for morphology, size distribution, encapsulation efficiency, magnetic property and *in vitro* release.

2. Materials and Methods

2.1. Materials

The pure sample of powdered Sulforaphane (SFP) was obtained from Vanco Herbals Solan, Himachal Pradesh, India as a compliment sample. Chemicals such as Pluronic P123, Conc. HCl, TEOS (Tetra ethyl ortho silicate), Hexane, Ethyl Alcohol and Butanol were obtained from Aman Scientifics. Iron, acetyl acetone, ammonium hydroxide, CTAB (Cetyl trimethyl ammonium bromide) and nitric acid (HNO_3) were obtained from Cros ChemicalsPvt Ltd.

2.2. Methods

In this current study, prepared four Sulforaphane-loaded magnetic nanoparticles by the calcified co-precipitation methods. Four types of MNPs were prepared as per the formula given in Table 1. The ingredients mentioned in part I were weighted and the contents were subjected to stirring over night at 32°C. Then the contents were transferred to container bottle made of teflon and heated the mixture to 100°C for 2 days. After this step the contents were subjected to straining and the obtained marc or precipitate was then washed (double distilled water only) and then dried. After drying the contents were subjected to calcination for 8 hr at 500°C.The specified quantities of ingredients such as Iron, acetyl acetone, nitric acid as per the formulations were mixed gently and heated at 80°C (The quantities of above mentioned ingredients were shown in Table 1).This process is continued for 4 hr. The nanoparticles were suspended overnight in the above mixture with occasional stirring to remove excess solvent. Then the resultant mixture was subjected to heating to 500°C using furnace for 2 hr with incremental effect i.e increasing the temperature of 2°C per minute [26, 27].

2.2.1. Preparation of Sulphoraphane MNPs by Encapsulation Technique

A specified amount of (0.4 g) iron silica (Fe-SiO_2), Fe-KIT-6, Fe-MCM-41, and Fe-SBA-15 were weighed (coded as F_1, F_2, F_3, F_4, respectively), adding to a 20 ml solution of Sulforaphane-hexane (1.4g) and macerated with periodic stirring for 3 days. Then the mixture was subjected to centrifugation, filtration followed by washing with hexane to obtain Sulforaphane MNPs. Obtained MNPs were subjected to vacuum drying for 10 hr at 60°C.

Table 1. Preparation of Four Magnetic Nanoparticles

Part	Name of the Ingredient	Quantity for Formulation			
		F_1	F_2	F_3	F_4
1	Pluronic-123 (gm)	1.4	-	1.23	0.17
	Concentrated Hydrochloric Acid (mL)	2.7	-	2.25	2.9
	Ethanol (mL)	6	-	-	-
	Tetra Ethyl Ortho Silicate (TEOS, mL)	5.2	10	10	1.09
	Cetyl Trimethyl Ammonium Bromide (CTAB, gm)	-	2.4	-	-
	Ammonium Hydroxide (mL)	-	8	-	-
	Deionized Water (mL)	-	120	44	202.6
2	Iron (gm)	0.3153	0.3153	0.3153	0.3153
	Acetyl Acetone (mL)	3	3	3	3
	Nitric Acid (mL)	0.3	0.3	0.3	0.3
	Silicon Di Oxide (gm)	0.25	-	-	-
	MCM-41 (gm)	-	0.25	-	-
	KIT-6 (gm)	-	-	0.25	-
	SBA-15 (gm)	-	-	-	0.25
3 Encapsulation	Sulforaphane (gm)	1.4	1.4	1.4	1.4

2.2.2. Evaluation or Characterization of Sulforaphane MNPs

2.2.2.1. Drug Response Study

The easy-to-use, inexpensive characterization method known as UV-Visible spectroscopy (UV-Vis) is frequently employed to investigate compounds at the nanoscale. UV-Visible spectroscopy is an important instrument for identifying, testing, and characterization of compounds, as well as comparing the stability of nanoparticle colloidal solutions. Nanoparticles possess optical properties that are sensitive to size, shape, concentration, refractive index and agglomeration state close to the surface of nanoparticles. A UV-visible spectrophotometer is frequently used to assess the formation of MNPs in aqueous solution [28]. The absorption of samples was examined using a UV-Visible spectrophotometer at 202 nm.

2.2.2.2. Fourier Transform Infrared Spectroscopy (FTIR)

The surface adsorption of useful structures on nanoparticles can be studied by using FTIR, which is specifically employed for the identification of unknown compounds. Users can study a layer of nanoparticles coated at the attenuated total reflectance (ATR) element while concurrently altering the area above it, which is a benefit. It is commissioned to study the chemistry of magnetic nanoparticles [29]. These pellets have undergone FTIR spectrophotometric analysis. Then, the collected data were in a wave range of about 400–4000 cm^{-1}.

2.2.2.3. X-Ray Diffraction (XRD)

One among the most often employed methods for the standardization of nanoparticles is X-ray diffraction (XRD). XRD typically offers information on the structure, type of segment, lattice parameters, and grain size of a crystal. One advantage of XRD methods is that they result in statistically representative, volume-averaged readings. These values are often obtained from samples that have been dried and converted to powder form. Because it provides information on the typical dimensions of nanocrystals, it is utilized to determine the segment identification of crystalline substances. The X-Ray Diffractometer (XRD) was successfully used to understand the crystallographic behavior of the produced magnetic nanoparticles [30].

2.2.2.4. Thermal Gravimetric Analysis (TGA)

Thermal gravimetric analysis offers data on the mass of a sample as it varies with temperature over time. Thermogravimetric analysis (TGA) can be used to determine the amount of coating on the surface of the nanoparticle. Thermogravimetric analysis is used to measure temperature and changes in mass. It also allows for the calculation of the type and quantity of natural ligands in NP, taking into account the initial mass pattern. The particles were placed in an aluminium pan and heated at a rate of 10°C/min from ambient temperature (25°C) to 250°C [30].

2.2.2.5. High Resolution Scanning Electron Microscopy (HRSEM)

The morphology of the prepared MNPs was assessed by performing high resolution scanning electron microscopy (HRSEM). Deionized water was used for the dynamic mild scattering method to determine the average particle diameter of MNPs. With the aid of SEM, morphological characteristics were investigated [31].

2.2.2.6. Elemental Mapping

The elemental mapping depicts the pattern of element distribution. Energy Dispersive X-Ray Analysis (EDX), often known as EDS or EDAX, is an X-ray method for determining the chemical composition of things. It is being used to confirm the adsorption at the surface of MNPs. Applications include researching materials and products, troubleshooting, and using an EDX spectrum analyzer to employ and detect preformulation for elemental evaluation. A well-established method for identifying and quantifying the elemental compositions of a tiny material is energy dispersive X-ray spectroscopy (EDS). It generates a spectrum that shows the peaks associated with the fundamental composition of the analysed pattern [30].

2.2.2.7. Loading Efficiency

Drug loading performance is defined as the ratio of the amount of drug contained within the nanoparticle to the total amount of drug used in the formulation of the nanoparticles. Encapsulation performance is one of the most important characteristics in developing nanoparticle, indicating drug loading performance. To measure the sample absorbance, a UV-Visible spectrophotometer set to 202 nm was utilized. Loading efficiency was determined using following formula,

$$\textbf{Drug loading efficiency} = \{(W - W_D)/W_{MNP}\} \times 100$$

Where, W, W_D, W_{MNP} denote the initial weight of Sulforaphane, the weight of the Sulforaphane within the solution, and weight of the MNP respectively [32].

2.2.2.8. Zeta Potential (ζ)

Zeta potential assesses the charge balance of colloidal nanoparticles by measuring the "effective" electric powered charge at the nanoparticle surface. The electrophoretic mobility was determined using the Malvern Zetasizer 3 000 HSA (Malvern Instruments, UK) to determine the zeta potential, which reflects the electric charge on the particle surface and indicates the physical stability of colloidal systems. The sample was tested in double distilled water and corrected to a conductivity of 50 IS/cm with a 0.9% w/v sodium chloride solution. The pH ranged between 5.5 and 7.5, and the applied field strength was 20 V/cm [30].

2.2.2.9. Analysis of a Vibrating Sample Magnetometer (VSM)

A vibrating-sample magnetometer (VSM) is a magnetic-

characteristics measurement technique that is solely based on Faraday's Law of Induction. VSM is a flexible approach for determining a pattern's magnetic second while it vibrates perpendicular to a homogeneous magnetizing zone region. This approach may identify little changes such as 10^{-5} to 10^{-6} emu. Magnetic second data from samples may be obtained using the VSM approach. The sample is moved sinusoidally using an electromagnetic vibration device. The sample moves in the magnetic field created by the excitation coils. As a result, a voltage is generated in a measuring coil, allowing the magnetic moment of the sample to be calculated. The VSM curve was created by plotting the applied magnetic field on the abscissa and the resulting mass magnetization or specific magnetization on the ordinate [30].

2.2.2.10. Colloidal Stability of Sulforaphane MNPs

The Sulforaphane MNPs were diluted to 1 mg/mL concentration by treating them with deionized water. Stability was determined on the basis of particle size. This test was conducted for 1 week using Dynamic Light Scattering method (DLS). The temperature maintained during this test period is constant and at 37°C. The colloidal stability was determined using following formula [31].

$$\textbf{Colloidal Stability } (t_n) = \frac{\textbf{Nanoparticle Size } t_n}{\textbf{Initial Nanoparticle size } t_0} X \ \textbf{100}$$

2.2.2.11. Dissolution Study *In-vitro*

The in-vitro dissolution study was carried out using standard test protocols, with three dissolution media selected based on their pH levels (pH 5.5, 6.5, and 7.4). The drug release study was carried out using a USP Type II apparatus. Standard conditions include a temperature of 37±0.5°C and agitation rate of 100 rpm [32]. This test was conducted on both the Sulphoraphane pure drug and the MNP. The samples were collected at specific time intervals (0, 2, 4, 8, 12, 16, 20, 24, 30, 36 hours), implemented a filtering process to the collected samples to reduce variation when calculating absorbance. Samples have been diluted with freshly prepared buffer to reduce concentration. The amount of drug released was measured using a UV-visible spectrophotometer at 202 nm [31].

3. Results and Discussion

The prepared Sulphoraphane (SFP) MNPs were characterized for the morphology, size distribution, bioavailability, stability, and dissolution.

The overlap of the Fe_2O_3 and SFP absorption bands resulted in maximum absorption at 202 nm. The drug response investigation confirmed that there is surface contact between iron nanoparticles and silica materials. This is explained by charge transfer and the additional support provided by the iron clusters on the silicas. UV-Vis spectrum was shown in Figure 1.

The FTIR study results reveals that there is compatibility between drug with formulation additives. It was confirmed by observing characteristic peak in spectra. The characteristic peaks such as 3415, 2924, 1645 cm^{-1} for O-H, C-H, C=C stretching vibrations, respectively (Figure 2). Similarly 1139, 1158 cm^{-1} for C-H bending (in-plane) and C−H vibrations respectively. The absorption peak of the prepared nanoparticles has not differ significantly. Also, the broad bands detected at 1139 cm^{-1} and 1158 cm^{-1} can be due to the C-groups vibrations and interactions with the NPs [33].

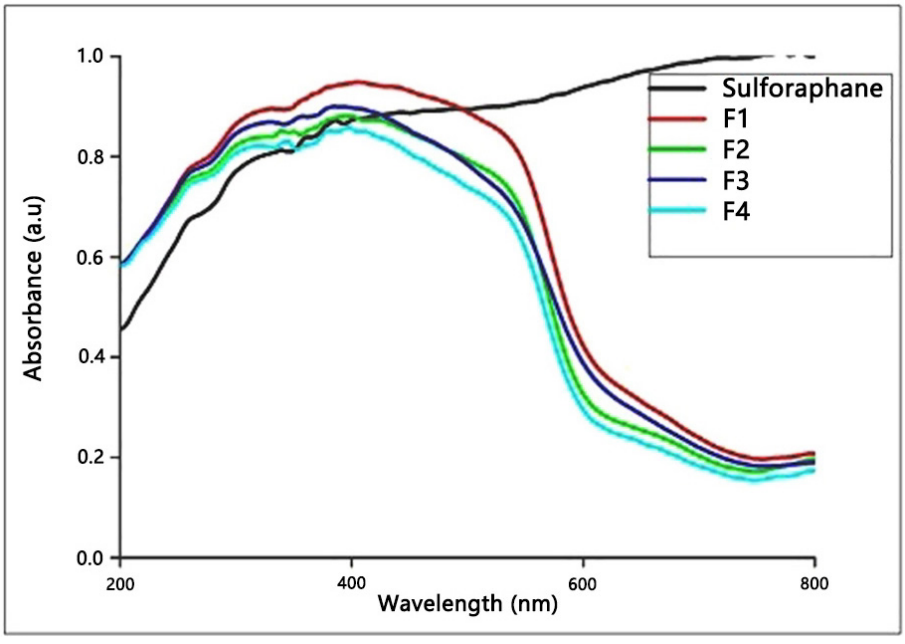

Figure 1. UV Spectrum of Sulforaphane loaded MNPs

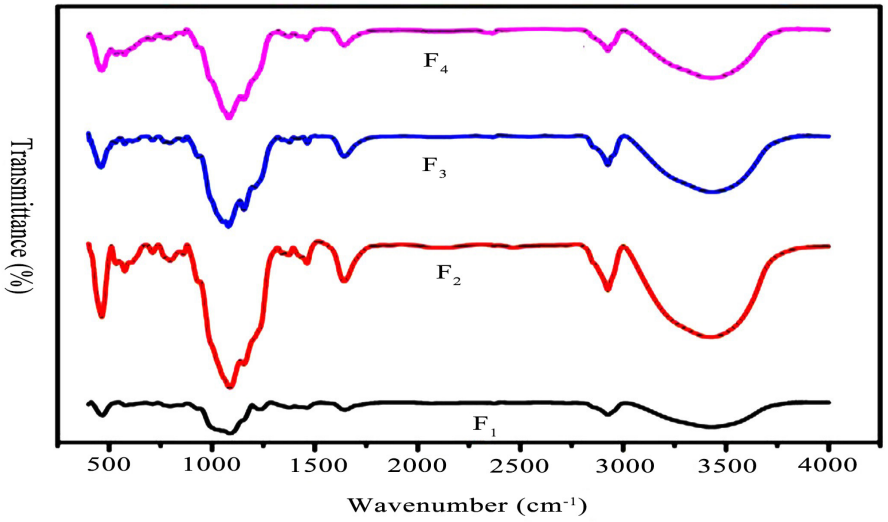

Figure 2. FT-IR spectrum of SFP Magnetic nanoparticles

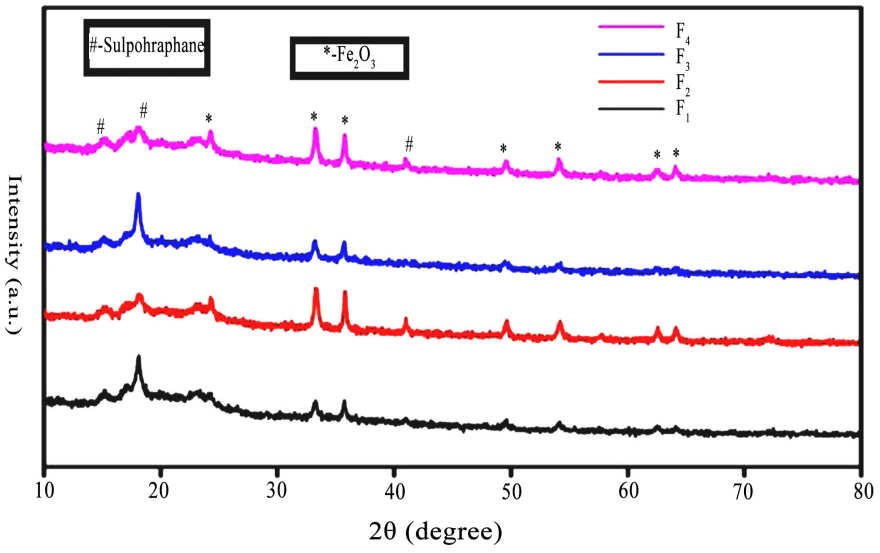

Figure 3. XRD graphs of SFP MNPs

In the XRD investigation, the distinctive peaks at 14.9°, 18.2° and 41.0° were detected in SFP and also in MNP formulations (shown in Figure 3). The diffraction peaks illustrate the highly crystalline nature of the particles. No XRD detectable impurities were observed in this sample as well. These findings demonstrated that all of the prepared MNPs had been successfully loaded with drug [34].

In TGA study, weight loss happens in two stages between 200 and 750 °C. Under 200 °C, the initial weight loss seen can be attributed to the elimination of absorbed water from the substance as well as the breakdown of the medicine in the material. Dehydroxylation from the surface silanol group (Si-OH) is responsible for the weight loss between 250°C and 750°C. (Figure 4). With Formulation F_4 (containing SBA-15), weight loss seems to be less than with other materials. The curve also indicated that no complex formation took place between drug molecules and polymer but they bind due to the electrostatic interactions [35].

According to a High Resolution Scanning Electron Microscopy (HRSEM) investigation, the materials have an uneven form and spherical morphology as a result of the medication being loaded onto nanoparticles made of silica components. Because the holes in the blood arteries in the tumor regions are larger, nanoparticles smaller than 200 nm stay longer in the blood circulation and have a tendency to collect in that region [29, 30]. The size range from 100 nm to 250 nm, which has an ideal size range, was obtained from the graph of SEM analysis of all MNPs with and without loading SFP. The HRSEM images were shown in Figure 5. Among all formulations, Formulation F_2 (Containing MCM-41), F_4 (Containing SBA-15) had a good aesthetic and the ideal size range.

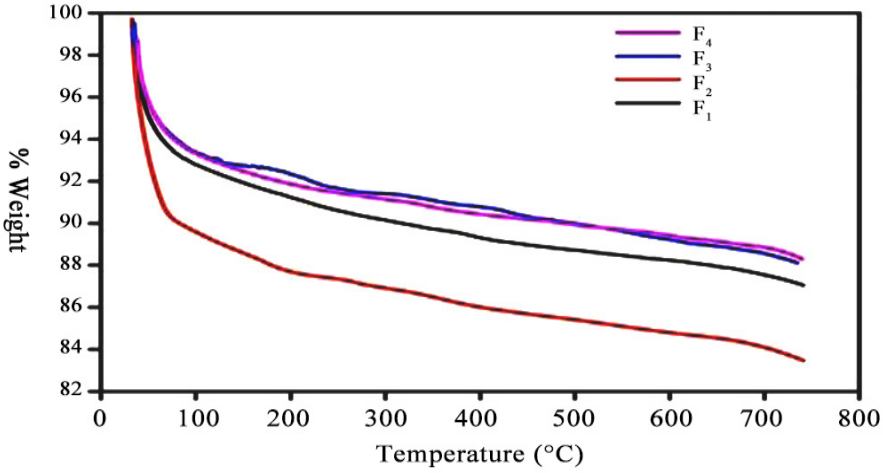

Figure 4. TGA analysis of Sulforaphane Magnetic nanoparticles

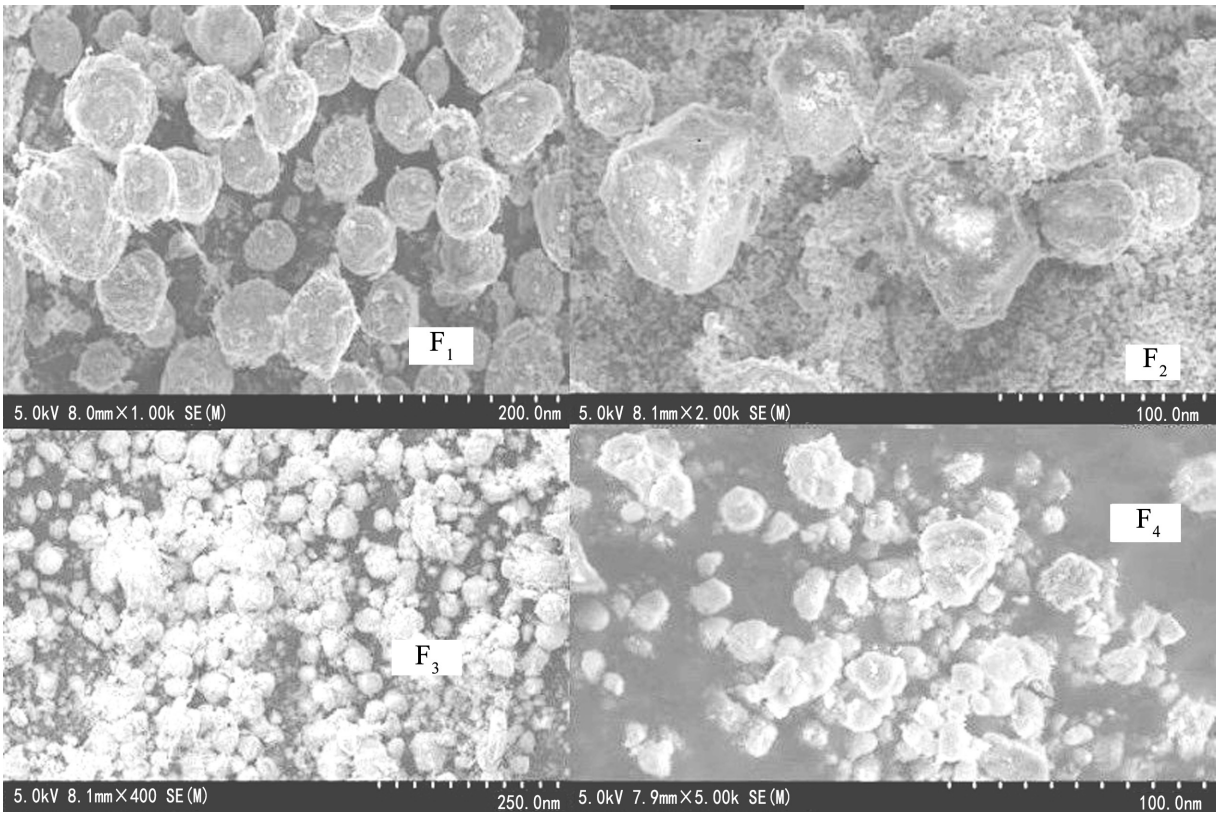

Figure 5. SEM images for all Formulations

The elemental mapping analysis was used to confirm the presence of C, Fe, Si, F, Cl, and O on the surfaces of the samples. The elemental compositions observed confirm the success of the synthesis as reported by other studies [36]. Table 2 shows the atomic percentages of all the catalysts based on EDX analysis in a micrometer range scanning.

The volume ratio of the aqueous and organic phases, the type of surfactant, and other factors all affect loading efficiency. Only a few of the governing parameters in this situation were optimized. The loading effectiveness of four SFP loaded MNPs was determined, and the results are displayed in Figure 6, indicating that SFP/MCM-41 (F_2) has a higher percentage (98%) when compared with other formulations.

Table 2. Elemental Mapping of Sulforaphane loaded MNPs

Magnetic Nano Particle Formulation (MNPs)	Elemental (%)					
	C	O	F	Si	Cl	Fe
F_1 .(Fe-SiO_2)	21.98	35.64	18.45	16.55	0	7.40
F_2 .(Fe-MCM-41)	29.24	40.20	4.40	14.12	0.91	11.05
F_3 .(Fe-KIT-6)	23.32	30.56	29.32	11.52	0	5.33
F_4 .(Fe-SBA-15)	31.09	42.29	10.01	11.17	0.23	6.11

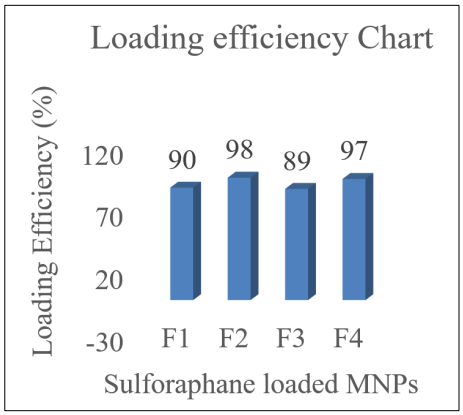

Figure 6. Loading efficiency of SFP loaded Magnetic nanoparticles

The loading efficiency (%) and colloidal stability percentage data are shown in Table 3.

Table 3. Sulforaphane-loaded MNPs' Loading Efficiency and Colloidal Stability

Formulation (MNPs)	Loading Efficiency (%, n=3)	Colloidal Stability (%)	
		1st Day	2nd Day
F_1	90±1.2	100	88±2.0
F_2	98±0.9	100	92±1.1
F_3	89±2.1	100	86±2.3
F_4	97±1.7	100	90±0.9

Zeta potential also contributes significantly to the stability and penetration of drugs. The Fe-MCM-41 MNP (F_2) has a negative charge due to the presence of iron molecules. Additionally, due to minimal protein binding on the surface of the particles, negative zeta potential is more favorable for the enhanced permeability and retention (EPR) effect as well as escape from identification by the immune system and phagocytic system, i.e. macrophages [37].

Based on the estimated zeta potential values, electrostatic stabilization was observed within the pH range of 3 to 11.

Figure 7 shows the end result of SFP/MCM-41 (F_2) nanoparticles, which have a positive charge due to the presence of stabilized drug (sulforaphane).

VSM provided the hysteresis curve of magnetic nanoparticles.

Figure 8 shows that the synthesized Fe-MCM-41MNP (F_2) has an ideal particle size of 50 nm, zero remanence and coercivity, implying super para magnetic activity, and may be magnetized when subjected to a magnetic field. It was established that the synthesized MNPs were extremely magnetic (super-paramagnetic). For numerous disorders, this trait is a desired characteristic in biomedical applications. Due to its small particle size and high surface area to volume ratio, loaded magnetic nanoparticles can be employed successfully for diagnostic, imaging, and therapy [37]. Figures 9-11 show the data obtained for the dissolution rate study.

The findings show that SFP loaded MNPs have a higher drug release than pure SFP with a larger surface area, which increases bioavailability. Among all four MNP formulations of SFP, the only formulation that satisfies the requirements for a prototype MNP is F_2. The pH of the medium has an inverse relationship with the amount of Sulphoraphane released by the MNP. The following is the order of dissolution (based on the percent cumulative drug release) pH 5.5>pH 6.5>pH 7.4. The cancer environment has an acidic pH in comparison to blood and healthy tissues, which is a well-known phenomenon. As a result, cancer therapy may benefit from SFP increased release in the tumor [38].

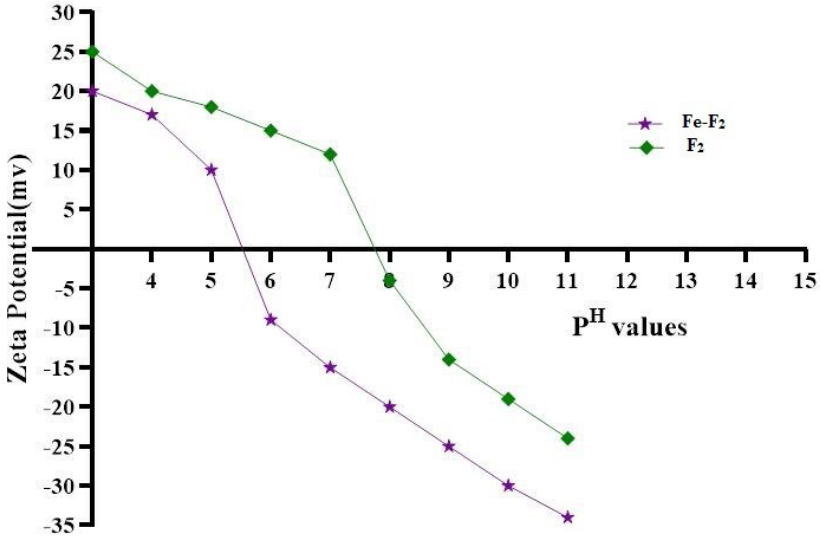

Figure 7. Comparative zeta potential plot for Fe-F_2, F_2

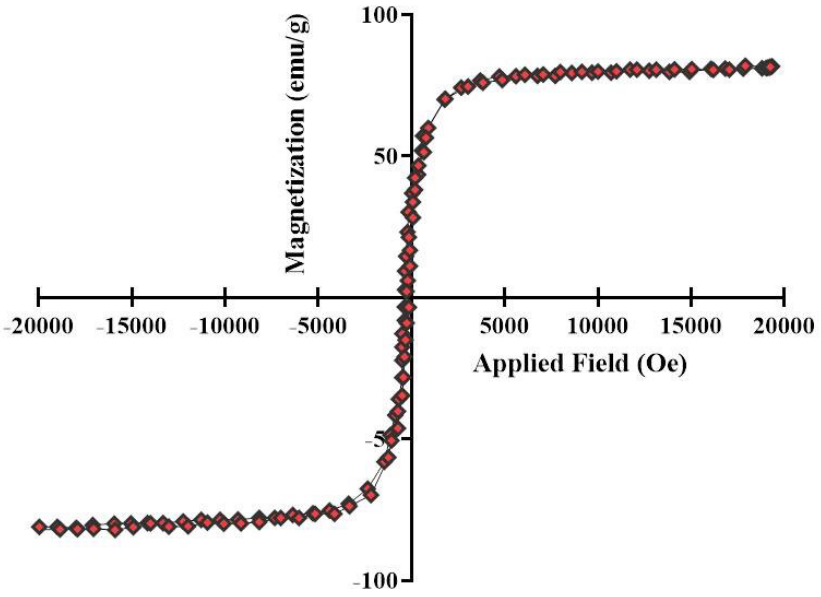

Figure 8. Magnetism of a Vibrating Sample of Fe - MCM - 41 MNP

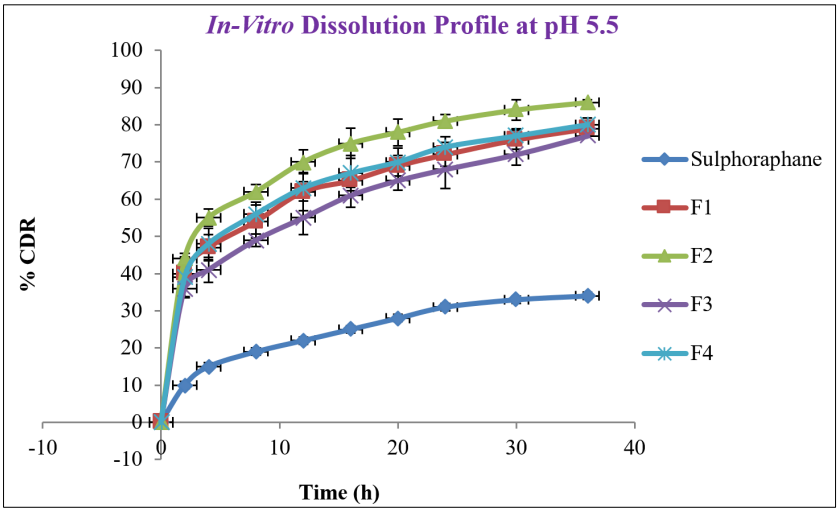

Figure 9. Dissolution study for Sulforaphane MNPs at pH 5.5

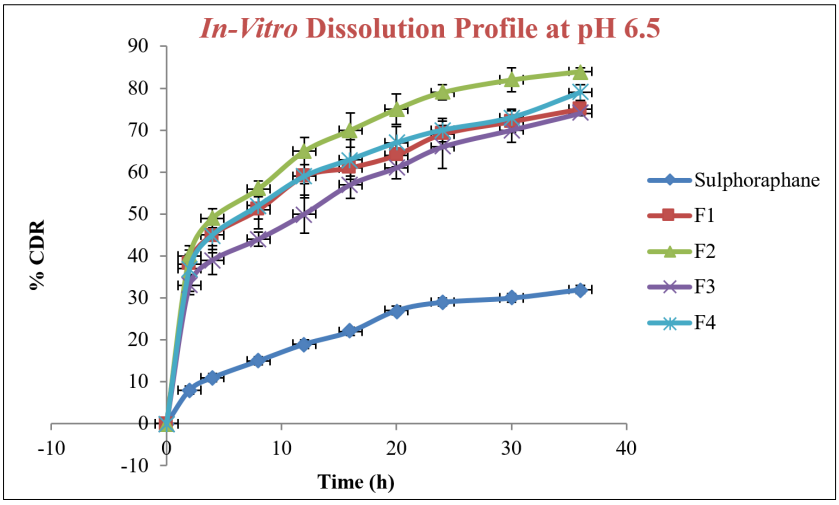

Figure 10. Dissolution study for Sulforaphane MNPs at pH 6.5

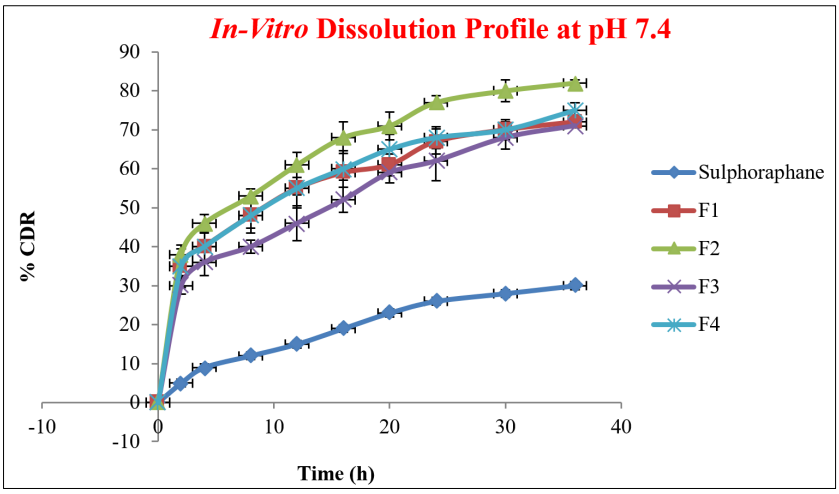

Figure 11. Dissolution study for Sulforaphane MNPs at pH7.4

4. Conclusions

Using the Pluronic block co-polymer P123 as a surfactant template, four different mesoporous Magnetic Nanoparticles for Sulforaphane were prepared incorporating iron oxides using a simple co-precipitation method. The formulations were characterized for drug response study, XRD, FTIR, Thermal Analysis, High Resolution Scanning Electron Microscopy (HRSEM), Colloidal Stability, *in-vitro* drug dissolution rate study and Loading Efficiency. According to the Drug Response Study, Sulforaphane has the highest absorbance at 202 nm and dissolution study of Sulforaphane loaded MNPs of Fe-MCM-41 (F_2) showed maximum drug release at pH 5.5. From the results, the study concluded that all the formulated magnetic nanoparticles are in aggregated morphology and were composed of smaller grains in nano size range with superparamagnetic properties, which exhibit magnetic responsiveness which is sufficient for drug targeting in the presence of an external magnetic field, and a large surface area and can be useful for the effective management of cancer.

Conflict of Interest

All authors declare no conflict of Interest.

Acknowledgments

Authors acknowledge sincere thanks to the Management of all participating Institutions for the facilities granted and constant encouragement for the completion of current research investigation.

REFERENCES

[1] Meir Djaldetti., “Sulforaphane: The Principal Broccoli

Phytochemical as a Cancer Challenger," Recent Progress in Nutrition, vol. 2, no. 1, pp. 1-7, 2022. DOI: 10.21926/rpn.2201008.

[2] Liu P., Atkinson S.J., Akbareian SE., "Sulforaphane exerts anti-angiogenesis effects against hepatocellular carcinoma through inhibition of STAT3/HIF-1α/VEGF signalling," Scientific Reports, vol. 7, Article ID. 12651, 2017. DOI: 10.1038/s41598-017-12855-w

[3] Alena Vanduchova, "Pavel Anzenbacher., and Eva Anzenbacherova., Isothiocyanate from Broccoli, Sulforaphane, and Its Properties," Journal of Medicinal Food, vol. 22, no. 2, pp. 121-126, 2019. DOI: 10.1089/jmf.2018.0024.

[4] Su X., Jiang X., Meng L., Dong X., Shen Y., Xin Y., "Anticancer Activity of Sulforaphane: The Epigenetic Mechanisms and the Nrf2 Signaling Pathway," Oxidative Medicine and Cellular Longevity, vol. 6, Article ID. 5438179, 2018. DOI: 10.1155/2018/5438179.

[5] Cinzia Calcabrini., Francesca Maffei., Eleonora Turrini and Carmela Fimognari., "Sulforaphane Potentiates Anticancer Effects of Doxorubicin and Cisplatin and Mitigates Their Toxic Effects," Frontiers in Pharmacology, vol. 11, Article ID. 567, 2020. DOI: 10.3389/fphar.2020.00567

[6] Rizwanullah M., Ahmad J., Amin S., "Nanostructured lipid carriers: a novel platform for chemotherapeutics," Current Drug Delivery, vol. 13, no. 1, pp. 4-26, 2016. DOI: 10.2174/1567201812666150817124133

[7] Rizwanullah M., Amin S., Ahmad J., "Improved pharmacokinetics and anti-hyperlipidemic efficacy of rosuvastatin-loaded nanostructured lipid carriers," Journal of Drug Targeting, vol. 25, no. 1, pp. 58-74, 2017. DOI: 10.1080/1061186X.2016.1191080

[8] Piazzini V., Lemmi B., Ambrosio M., Cinci L., Luceri C., Bilia AR., Bergonzi MC., "Nanostructured lipid carriers: promising drug delivery systems for plant extracts: The Case of Silymarin," Applied Science, vol. 8, no. 7, Article ID. 1163, 2018. DOI: 10.3390/app8071163

[9] Ling G., Zhang T., Zhang P., "Nanostructured lipid-carrageenan hybrid carriers (NLCCs) for controlled delivery of mitoxantrone hydrochloride to enhance anticancer activity bypassing the BCRP mediated efflux," Drug Development and Industrial Pharmacy, vol. 42, no. 8, pp. 1351–59, 2016. DOI: 10.3109/03639045.2015.1135937

[10] LuAH., Schmidt W., "Nanoengineering of a Magnetically Separable Hydrogenation Catalyst," Angewandte Chemie, vol. 43, no. 33, pp. 4303-4306, 2014. DOI: 10.1002/anie.200454222

[11] Arias LS., Pessan JP., Vieira APM., Lima TMT., Delbem ACB., Monteiro DR., "Iron Oxide Nanoparticles for Biomedical Applications: A Perspective on Synthesis, Drugs, Antimicrobial Activity, and Toxicity," Antibiotics (Basel), vol. 7, no. 2, Article ID. 46, 2018. DOI: 10.3390/antibiotics7020046.

[12] Ramaswamy B., Kulkarni SD., Villar PS., "Movement of magnetic nanoparticles in brain tissue: mechanisms and impact on normal neuronal function. Nanomedicine: Nanotechnology," Biology and Medicine, vol. 11, no. 7, pp. 1821-1829, 2015. DOI: 10.1016/j.nano.2015.06.003

[13] He Le., Wang Mingsheng., "Magnetic Assembly Route to Colloidal Responsive Photonic Nanostructures," Accounts of Chemical Research, vol. 45, no. 9, pp. 1431-1440, 2012. DOI: 10.1021/ar200276t

[14] Kavre Ivna., Kostevc Gregor., "Fabrication of magneto-responsive microgears based on magnetic nanoparticle embedded PDMS," RSC Advances, vol. 4, no. 72, pp. 38316-38322, 2014. DOI: 10.1039/c4ra05602g

[15] Mornet S., Vasseur S., Grasset F., "Magnetic nanoparticle design for medical applications," Progress in Solid State Chemistry, vol. 34, no. 4, pp. 237-247, 2006. DOI: 10.1021/cr300068p

[16] Gleich B., Weizenecker J., "Tomographic imaging using the nonlinear response of magnetic particles," Nature, vol. 435, no. 7046, pp. 1214-1217, 2005. DOI: 10.1038/nature03808

[17] Bo Shen., Shouheng Sun, "Chemical Synthesis of Magnetic Nanoparticles for Permanent Magnet Applications," Chemistry Europe, vol. 26, no. 30, pp. 6757-6766, 2020. DOI: 10.1002/chem.201902916

[18] Kateryna Loza, Marc Heggen, Matthias Epple, "Synthesis, Structure, Properties, and Applications of Bimetallic Nanoparticles of Noble Metals," Advanced Functional Materials, vol. 30, no. 21, Article ID. 1909260, 2020. DOI: 10.1002/adfm.201909260

[19] Philip J., Shima PD., Raj B., "Nanofluid with tunable thermal properties," Applied Physics Letters, vol. 92, no. 4, Article ID. 043108, 2008. DOI: 10.1063/1.2838304

[20] Chaudhary V., Wang Z., Ray A., "Self-pumping magnetic cooling, Journal of Applied Physics, vol. 50, no. 3, Article ID. 03LT03, 2016. DOI: 10.1088/1361-6463/aa4f92

[21] Mahendran V., "Nano fluid based optical sensor for rapid visual inspection of defects in ferromagnetic materials," Applied Physics Letters, vol. 100, no. 7, Article ID. 073104, 2012. DOI: 10.1063/1.3684969

[22] Chaudhary V., Ramanujan RV., "Magneto caloric Properties of Fe-Ni-Cr Nanoparticles for Active Cooling, Scientific Reports, vol. 6, no. 1, Article ID 35156, 2016. DOI: 10.1038/srep35156

[23] Philip V., Felicia., Leona., "A Simple, In-Expensive and Ultrasensitive Magnetic Nano fluid Based Sensor for Detection of Cations, Ethanol and Ammonia," Journal of Nanofluids, vol. 2, No. 2, pp. 112-119, 2013. DOI: 10.1166/jon.2013.1050

[24] Muge Yılmaz., Ozgul., "Synthesis and characterization of MCM-41 with different methods and adsorption of Sr^{2+}on MCM-41," Research on Chemical Intermediates, vol. 41, no. 6, pp.199-211, 2015. DOI: 10.1007/s11164-013-1182-4

[25] Wei Wang., "Synthesis of KIT-6 type mesoporoussilicas with tunable pore sizes, wall thickness and particle sizes via the partitioned cooperative self-assembly process," Microporous and Mesoporous Materials, vol. 5, no. 1, pp. 194-206, 2013. DOI: 10.1016/j.micromeso.2013.10.028

[26] Zhou B., Li C., Jiang M., "Pore structure of mesoporous silica (KIT-6) synthesized at different temperatures using positron as a non-destructive probe," Applied Surface Science, vol. 450, pp. 31-37, 2016. DOI: 10.1016/j.apsusc.2018.03.223

[27] Song SW., Hidajat K., Kawi S., "Functionalized SBA-15

Materials as Carriers for Controlled Drug Delivery: Influence of Surface Properties on Matrix-Drug Interactions," Langmuir, vol. 21, no. 21, pp. 9568-9575, 2015. DOI: 10.1021/la051167e

[28] Kriti Soni., Rizwanullah MD., "Development and optimization of sulforaphane loaded nanostructured lipid carriers by the Box- Behnken design for improved oral efficacy against cancer: in vitro, ex vivo and in vivo assessments," Artificial Cells, Nanomedicine and Biotechnology, vol. 46, no. 1, pp. 15-31, 2018. DOI: 10.1080/21691401.2017.1408124

[29] Kumari M., Sharma N., Manchanda R., "PGMD/curcumin nanoparticles for the treatment of breast cancer," Scientific Reports, vol. 11, no. 1, pp. 1-17, 2021. DOI: 10.1038/s41598-021-81701

[30] Stefanos Mourdikoudis., Roger M., Pallares and Nguyen T. K. Thanh, "Characterization techniques for nanoparticles: comparison and complementarity upon studying nanoparticle properties," Nanoscale, vol. 10, Article ID. 12871, 2018. DOI: 10.1039/C8NR02278J

[31] Rashid Roni MS., Guanguan N., "The Effects of pH on the Structure and Bioavailability of Imidazobenzodiazepine-3-Carboxylate MIDD0301," Molecular Pharmaceutics, vol. 17, no. 4, pp. 1182-1192, 2020. DOI: 10.1021/acs.molpharmaceut.9b01210

[32] Hao Zhu., Xiaomei Chen., Mariam Ahmed., "Proposal of Conducting Bioequivalence Trials with Gastric pH Modulators for Two Oral Formulations Demonstrating Different Dissolution Profiles at Elevated pH," Clinical and Translational Science, vol. 12, no. 6, pp. 564-572, 2019. DOI: 10.1111/cts.12658

[33] Jadia Kydd., Rai P., "Remotely photo triggered, transferrin-targeted polymeric nanoparticles for the treatment of breast cancer," Photochemistry, Photobiology, vol. 4, no. 4, pp. 765-774, 2018. DOI: 10.1111/php.12903

[34] Nydeia WB., Vijaya KR., Shaik Jeelani., Seyhan Boyoglu., Shree RS., "Synthesis and Evaluation of Magnetic Nanoparticles for Biomedical Applications," Journal of Nanoparticles, vol. 2013, Article ID. 370812, 2013. DOI: 10.1155/2013/370812.

[35] Kavita Tayal, Gurpreet Kandav, Priti Girotra, Shailendra Kumar Singh, "Formulation and evaluation of chitosan coated magnetic nanoparticles of Amoxicillin trihydrate," Der Pharmacia Lettre, vol. 7, no. 11, pp. 241-251, 2015.

[36] Hariani PL., Faizal M., Ridwan R., Marsi M., Setiabudidaya D., "Synthesis and properties of Fe3O4 nanoparticles by co-precipitation method to removal procion dye," International Journal of Environmental Science and Development, vol. 4, no. 3, pp. 336-340, 2013. DOI: 10.7763/IJESD.2013.V4.366

[37] Lazhen Shen., Yongsheng Qiao., Yong Guo., Shuangming Meng., Guochen Yang., Meixia Wu., Jianguo Zhao., "Facile co-precipitation synthesis of shape-controlled magnetite nanoparticles," Ceramics International, vol. 40, no. 1, pp. 1519-1524, 2014. DOI: 10.1016/j.ceramint.2013.07.037

[38] Gillies RJ., Raghunand N., Karczmar GS., Bhujwalla ZM., "MRI of the tumor microenvironment," Journal of Magnetic resonance Imaging, vol. 16, no. 4, pp. 430-450, 2002. DOI: 10.1002/jmri.10181.